Changes of Extreme Climate Indices on the Mongolian Plateau during 1981-2020 Based on ERA5 Reanalysis

Guoying Zhu
Peking University
Xinyi Zhao (sh-zhao@urban.pku.edu.cn)
Peking University

Research Article

Keywords: Mongolian Plateau, Extreme climate, ERA5, Atmospheric circulation indices, Inter-decadal variation

Posted Date: April 12th, 2023

DOI: https://doi.org/10.21203/rs.3.rs-2800110/v1

Additional Declarations: No competing interests reported.

Version of Record: A version of this preprint was published at Theoretical and Applied Climatology on July 22nd, 2023. See the published version at https://doi.org/10.1007/s00704-023-04567-1.

Abstract

The Mongolian Plateau (MP) is susceptible to extreme climate events due to its unique geographical location and socio-economic conditions. The focus of this study was to analyze the changes in extreme climate indices on the MP based on the ERA5 reanalysis dataset, as well as to investigate the relationship between these indices and atmospheric circulation indices. 1) Results indicated that the inter-annual variation trends of Summer days, Warm days, and Warm nights have significantly increased across the entire MP, with the central region experiencing a higher probability of extreme hot events. The inter-decadal variation of extreme hot indices rose the fastest from period 2 (1991-2000) to period 3 (2001-2010). 2) Results showed a substantial decrease in extreme cold events throughout the study period, with the most rapid decrease observed from period 1 (1981-1990) to period 2 (1991-2000), except for Frost days. 3) There was a decrease in extreme wet indices from 1981-2020. The Simple Precipitation Intensity Index (SDII) and Total precipitation in wet days (PRCPTOT) exhibited a significant descending trend in the northern and northeastern MP. Decadal variations showed a decrease in extreme precipitation, with the most significant decline observed between period 2 (1991-2000) to period 3 (2001-2010). 4) Extreme precipitation indices indicate a negative correlation with the Atlantic Meridional Mode (AMM). The Arctic Oscillation (AO) displayed a negative correlation with extreme cold indices, whereas the Pacific Decadal Oscillation (PDO) demonstrated a negative correlation with extreme hot indices.

1 Introduction

It is widely known that global warming has become a concern in the 21st century. According to the Sixth Assessment Report (AR6) of the Intergovernmental Panel on Climate Change (IPCC), the intensity and frequency of climate extremes have increased since pre-industrial times (Seneviratne et al. 2021). Climate model results also indicate that high-temperature extremes and heavy precipitation will occur more frequently in the future (Easterling et al. 2000), which means that the frequency of hazards induced by climate extremes will increase as well. It is also found that the possibility of climate extreme occurrences depends on the rate of warming rather than the warming level (Fischer et al. 2021).

Analyzing climate extremes is crucial for gaining a better understanding of their underlying mechanisms and providing valuable information for policymakers. Over 70% of the land on Earth has shown an increasing trend in high-temperature extremes and a decreasing trend in low-temperature extremes. Precipitation extremes have also exhibited a large-scale increasing trend, although their spatial coherence is not as pronounced as that of temperature extremes(Alexander et al. 2006).

Researchers have drawn similar conclusions in many regions and sub-regions. In Europe, it is observed that extreme high temperature and low temperature have risen by 2.3℃ and more than 3 ℃, respectively, from 1950 to 2018 (Lorenz et al. 2019). Based on the output of climate models, it's projected that the frequency and intensity of heat waves will increase by the end of the 21st century in Europe (Beniston et al. 2007). In Asia, the change of climate extremes has been found in many sub-regions. Temperature indices such as the annual maximum of daily maximum and minimum temperature increased from

1950–2003 in the Middle East, while precipitation indices didn't show a significant trend and spatial coherence (Zhang et al. 2005). It has been found the frequency of heavy rainfall and extreme heavy rainfall events increased over Greater Mumbai, India (Mann et al. 2023). In eastern Asia, an increase in the frequency and intensity of warm extremes have been observed in most parts of China and Northern China, respectively (Fu et al. 2013). Compared with 1960–1989, The frequency of cold extremes increased in North China and Northeast China in 1990–2007 (Xu et al. 2011). An increasing trend in precipitation intensity and magnitude has been found in most regions of China(Zhang and Zhao 2022). It's detected that the frequency and amount of extreme precipitation increased in South China, Southeast Asia, and North China and decreased in the Yangtze River basin (Cui et al. 2019). The change of climate extremes has also been found in many other regions in the world, such as South America, Africa, and Australia (Mason et al. 1999, Fu et al. 2010, Rusticucci 2012, Kruger and Sekele 2013).

The impact of climate extremes might be catastrophic (Kemp et al. 2022), affecting human health, destroying infrastructure, and causing economic losses (Bell et al. 2018). According to existing research, the exceptionally high temperature would lead to more mortality than in moderate conditions (Hajat et al. 2006, Roldán et al. 2014). Extreme temperature also causes illness directly and indirectly. A recent study shows chronic kidney disease is associated with high, low, and not-optimum temperature (He et al. 2022).

The Mongolian Plateau (MP) is located in the northeast of Asia and belongs to the semi-arid to the arid region. Its average altitude is 1580 m, and its average precipitation is around 250 mm. People inhabiting the MP make a living from herding. It's projected that extreme events will adversely affect the pastureland and water resources on the MP (Bayasgalan et al. 2006). When an arid summer or freezing winter comes, it will do great harm to the livestock and the local society. The severe winter is called dzud in the Mongolian language, a hazard including snowstorms and killing freeze in winter. Since 1950, the frequency and intensity of dzuds have been higher than before (Fernández-Giménez et al. 2012). Due to the dispersed population and specific geographical situation, people living on the MP are susceptible to climate extremes.

Some research has been conducted on the IMP. It is pointed out that the indices characterizing extreme low-temperature events decreased, and those describing extreme high temperature events increased in Inner Mongolia from the 1960s to 2010s, and the slopes have become steeper since the 1990s (Yan et al. 2014, Chen and Zhao 2017). The regional average of extreme precipitation indices shows a downtrend, and the trends of indices present significant spatial differences and inter-annual variation (You et al. 2010, Li et al. 2017, Chun et al. 2019). There will be more extreme precipitation in the dry area in the IMP (Li et al. 2018).

Some research focused on Mongolia or the entire MP. Almost all the extreme temperature indices show warming trends on the MP. The number of cool days and nights increases in all seasons, while the number of hot days and nights increases only in summer in Mongolia (Dashkhuu et al. 2015, Liu et al. 2019). The trends of the extreme temperature indices are consistent with the trends on other plateaus, such as the Loess Plateau and the Qinghai-Tibet Plateau (Du et al. 2013, Yan et al. 2015). The trends and

the spatial distribution of precipitation extremes seem to be more complex than those of the temperature, and the decadal precipitation shows a downtrend from east to west (Wang et al. 2016). Projections based on CMIP5 model output show that drought will happen more often under the RCP4.5 and RCP8.5 scenarios, and the drought in Mongolia will be more severe than that in Inner Mongolia (Li et al. 2020).

Over the past two decades, hazards caused by climate extremes have occurred many times, including the dzud of 2000–2002 and 2010(Fernández-Giménez et al. 2012, Iijima and Hori 2016), so it's of great importance to analyze the change of climate extremes over the whole MP. However, the spatial distribution of the meteorological stations on the MP is inhomogeneous. The stations in China are more intensive than those in Mongolia. Therefore, the ERA5 reanalysis dataset is applied in this study to make up for the sparse meteorological stations. This study aims to resolve the following three questions1) Use the ERA5 dataset to calculate extreme indices and analyze changes of extreme indices. 2) Investigate the relationship between extreme climate indices and circulation indices.

2 Datasets And Methods

2.1 Data

2.1.1 Data availability

The data sources utilized in this article comprised of meteorological station data and reanalysis datasets. The meteorological station data from the Inner Mongolia Autonomous Region were derived from China National Terrestrial Meteorological Station Basic Meteorological Element Day Value Data Set (V3.0) (1981–2020) and included temperature (maximum and minimum) and precipitation data from 94 stations in the region. The meteorological station data from Mongolia were obtained from the Global Historical Climatology Network - Daily (GHCN Daily) Version 3 (https://www.ncei.noaa.gov/access/metadata/landing-page/bin/iso?id=gov.noaa.ncdc%3AC00861), covering the time span of 1981.1-2020.12, and 40 stations were selected. The elevation of MP and spatial distribution of meteorological stations are shown in Fig. 1.

The reanalysis data used in this study were obtained from the European Centre for Medium-Range Weather Forecasts (ECMWF) ERA5 hourly data on single levels spanning from 1940 to present. This dataset has a spatial resolution of 0.25° and provides hourly estimates of dozens of variables on a global scale. Two variables, 2m temperature, and total precipitation were selected to calculate and analyze the extreme temperature and precipitation indices on the MP.

Atmospheric circulation indices were obtained from NOAA (https://psl.noaa.gov/data/climateindices/list/). At first we picked up 15 indices to investigate the relationship between extreme climate indices and atmospheric circulation indices and 4 indices were finally selected, including Atlantic Meridional Mode (AMM), Arctic Oscillation (AO), Pacific Decadal Oscillation (PDO), and Western Hemisphere Warm Pool (WHWP).

2.2 Methods

2.2.1 Theil-Sen slope and MK test

The Theil-Sen slope method is a robust non-parametric technique for estimating the slope of a linear relationship between two variables. Unlike ordinary least squares regression, the Theil-Sen slope method does not require any assumptions about the distribution of the data or the presence of outliers, and it can provide reliable estimates even when the data are highly skewed or contain extreme values. This method is suitable for trend analysis of long time series data. Theil-Sen slope is calculated as follows:

$$Slope = Median\left(\frac{x_i - x_j}{i - j}\right), \forall i > j$$

2.1

The MK trend test is a non-parametric statistical test that assesses whether there is a significant trend in the data over time. This test is particularly useful in situations where the data is not normally distributed or where the data does not meet the assumptions of traditional parametric tests. Z statistic is calculated as follows:

$$\mathrm{Z} = \begin{cases} \frac{S-1}{\sqrt{Var(S)}} S > 0 \\ 0 S = 0 \\ \frac{S+1}{\sqrt{Var(S)}} S < 0 \end{cases}$$

2.2

$$\mathrm{Var}\left(\mathrm{S}\right) = \frac{1}{18}\left[n\left(n-1\right)\left(2n+5\right) - \sum_{a=1}^{g} t_a(t_a-1)(2t_a+5)\right]$$

2.3

In (2.3), *g* is the number of tied groups, and t_a is the number of repetitions in tied group *a.*

$$\mathrm{S} = \sum_{j=1}^{n-1} \sum_{i=j+1}^{n} sgn(x_i - x_j)$$

2.4

In (2.4), sgn represents a mathematical function that gives the sign of a real number, as is shown in (2.5):

$$sgn\left(x_i - x_j\right) = \begin{cases} 1 x_i - x_j > 0 \\ 0 x_i - x_j = 0 \\ -1 x_i - x_j < 0 \end{cases}$$

2.5

2.2.2 Stepwise Regression

Stepwise regression is a statistical technique used to select the most relevant variables for predicting an outcome variable. It is an automated iterative procedure that enters or removes variables based on their contribution to the prediction model. This technique has gained popularity in recent years as it provides a more parsimonious and efficient way of modeling a large number of predictors. Stepwise regression was conducted using MATLAB.

2.2.3 Extreme climate indices

According to the Expert Team on Climate Change Detection and Indicators (ETCCDI), there are 27 core extreme indices that are based on daily temperature and precipitation. These indices include both fixed and percentage thresholds. In this article, sixteen extreme climate indices were selected for analysis, as listed in the Table 1.

Table 1
Definition of 16 extreme climate indices applied in this study

Indices	Abbreviation	Description	Unit
Summer days	SU25	Number of days when TX > 25℃	day
Tropical nights	TR20	Number of days when TN > 20℃	day
Warm days	Tx90p	Percentage of days when TX > 90th percentile	%
Warm nights	Tn90p	Percentage of days when TN > 90th percentile	%
Warm spell duration index	WSDI	Annual count of days with at least 6 consecutive days when TX > 90th percentile	day
Frost days	FD	Number of days when TN < 0℃	day
Icing days	ID0	Number of days when TX < 0℃	day
Cold days	Tx10p	Percentage of days when TX < 10th percentile	%
Cold nights	Tn10p	Percentage of days when TN < 10th percentile	%
Cold spell duration index	CSDI	Annual count of days with at least 6 consecutive days when TN < 10th percentile	day
Simple precipitation intensity index	SDII	Total precipitation in wet days (PRCP > 1mm) divided by count of wet days	mm/day
Total precipitation in wet days	PRCPTOT	Total precipitation in wet days (PRCP > 1mm)	mm
Consecutive dry days	CDD	Maximum length of dry spell, maximum number of consecutive days with RR < 1mm	day
Consecutive wet days	CWD	Maximum length of wet spell, maximum number of consecutive days with RR ≥ 1mm	day
Heavy precipitation days	R10mm	Annual count of days when PRCP ≥ 10mm	day
Heavy precipitation	R95p	Annual total PRCP when RR > 95th percentile	mm

2.1.2 Evaluation of ERA5 dataset

Site data was utilized to validate reanalysis data in a point-to-point grid. We process temperature and precipitation data as monthly averages and calculated root mean square error (RMSE), mean bias (MB), and correlation coefficient (CC) between station data and ERA5 reanalysis dataset. The calculation methods of all parameters are as follows:

$$\mathrm{RMSE} = \sqrt{\frac{1}{N}\sum_{i}^{n}\left(Obs_i - ERA_i\right)^2}$$

2.6

$$\mathrm{MB} = \frac{1}{N}\sum_{i}^{n}\left(Obs_i - ERA_i\right)$$

2.7

$$\mathrm{CC} = \frac{Cov(Obs, ERA)}{Var\left(Obs\right) Var\left(ERA\right)}$$

2.8

Obs_i is meteorological station data and ERA_i is ERA5 reanalysis dataset. Results are shown in Table 2 and Fig. 2. It can be found that there is a very good correlation between temperature and precipitation between observation data and reanalysis data, with CCs close to 1. MB values of average temperature (Taver), maximum temperature (Tmax), minimum temperature (Tmin) and precipitation (Pre) are 0.43℃, 1.41℃, -0.17℃ and − 10.07mm. The MB of temperature is within the range of ± 1.5 ℃, and the MB of precipitation is within the range of ± 15mm. RMSE values of Taver, Tmax, Tmin, and Pre are 0.63℃, 1.55℃, 0.68℃ and 12.83 mm. Combined with Fig. 2, ERA5 data slightly underestimates Tmax and has a certain degree of height for precipitation, but overall the simulation effect is fairly good. Based on the above analysis, ERA5 data can simulate the temperature and precipitation data of Mongolian Plateau well.

Table 2
Calculation results of CC, MB, and RMSE

	CC	MB	RMSE
Taver	1.00	0.43	0.63
Tmax	1.00	1.41	1.55
Tmin	1.00	-0.17	0.68
Pre	0.98	-10.07	12.83

3 Results And Discussion

3.1 The overview of temperature and precipitation on the Mongolian Plateau

In the context of global climate change, the temperature of the MP has also shown a significant upward trend in the past 40 years. Figure 3a) displays the raster-averaged annual maximum, mean, and minimum temperatures from 1981 to 2020 in the region of MP. All temperature measurements exhibited increasing trends, with rates of 0.40 ℃/decade, 0.37 ℃/decade, and 0.38 ℃/decade, respectively. Figure 3c) shows the spatial distribution of trends of average temperature during 1981–2020. Average temperature significantly increased during 1981–2020 on the almost entire MP at 0.05 confidence level and insignificantly decreased on small part of the southwestern MP. The rising trend of temperature on the central MP, where the Khangai mountains are located, is higher than that in other regions.

In Fig. 3b), the raster-averaged annual total precipitation in MP is presented, ranging from 240 mm to 400 mm during the 1981–2020 period. The change in annual precipitation appeared to be complex, increasing from 1980–1990, decreasing from 1990–2010, and then ascending again after 2010. Notably, precipitation levels in 2000–2010 were the lowest observed throughout the entire study period. In general, precipitation in the first two decades is more than that in the last two decades. Figure 3d) illustrates the spatial distribution of trends of total precipitation. Precipitation significantly decreased at 0.05 confidence level on the northern, northwestern and eastern MP and increased insignificantly on the southwestern MP. Northern and northeastern parts of the MP are facing more severe threat of water shortage.

3.2 Change of extreme climate indices

3.2.1 Extreme hot indices

The raster-averaged annual, decadal and trends of extreme indices on the MP were calculated. We applied Sen's slope method to calculate trends and MK test method to calculate the significant level of the trends. To investigate decadal changes of indices, we divided the research period into four equal periods calling period 1(1981–1990), period 2 (1991–2000), period 3(2001–2010), and period 4 (2011–2020), and calculated the difference between two adjacent periods.

Drought is a frequent climate threat on the MP, and Extreme hot events is an important factor leading to droughts. Besides, extreme hot events also do harm to human and livestock health. Here we select 5 indices to characterize extreme hot events, including Summer days (SU25), Tropical nights (TR20), Warm days (Tx90p), Warm nights (Tn90p) and Warm spell duration index (WSDI). Changes of extreme hot indices from 1981 to 2020 are shown in Fig. 4 and Theil-Sen Slope is shown in Table 3. Double asterisks mean the slope is significant at 0.05 confidence level. SU25 and TR20 are threshold-based indices, both increasing significantly with trends of 5.29 days/decade and 1.58 days/decade during 1981–2020. Tx90p and Tn90p calculate the percentage of days when the maximum temperature exceeds a certain percentage. Tx90p and Tn90p also increased with trends of 2.45%/decade and 2.7%/decade respectively during 1981–2020. WSDI calculate the maximum number of days that abnormal hot days lasts, significantly increasing with a trend of 1.41 days/decade. The degree of extreme heat events facing the MP has gradually increased over the past 40 years.

Table 3
Trends and inter-decadal variation of extreme hot indices

	period 1	period 2	period 3	period 4	Slope
SU25(day)	45.30	51.29	61.76	59.23	5.19**
TR20(day)	4.91	6.88	9.88	9.63	1.58**
TX90p(%)	6.89	9.98	12.72	13.52	2.45**
TN90p(%)	7.12	9.82	12.59	14.37	2.70**
WSDI(day)	0.92	3.03	4.80	5.04	1.41**

We further investigated the spatial variability of trends of these extreme heat indices.

Figure 5 shows the spatial pattern of trends of extreme hot indices (SU25, TR20, Tx90p, and Tn90p). The spatial pattern of the inter-annual variation trends of SU25, Tx90p and Tn90p is similar, increasing significantly on almost the entire MP. The magnitude of upward trends of these three indices in the central part of the MP is higher than those around the MP. Therefore, the probability of the central MP facing extreme hot events in the future is higher than that of other regions. Unlike the other three indices, TR only increased significantly in the southwestern MP, where deserts are located, and showed no obvious trend on other parts of the MP.

The decadal change of extreme hot indices is worth noting as well. According to the results in Table 3, nearly all the extreme hot indices rose the fastest from period 2 to period 3. SU25 and TR20 increased by 10.47 days and 3 days from period 2 to period 3. Tx90p and Tn90p increased by 2.74% and 2.77% from period 2 to 3. This means that the frequency of high temperature extremes increased the fastest in the decade 2001–2010 compared to 1991–2000.

We calculated the spatial difference of extreme hot indices between two adjacent periods and displayed it in Fig. 6. SU25 and Tx90p are indices that measure daytime high temperatures. From period 1 to period 2, the spatial differences in the changes of SU25 are not significant while the rise of Tx90p in the south of MP is significantly higher than that in other regions. From period 2 to period 3, SU25 mainly rises in the northeast of MP, while Tx90p mainly rises in the middle by west. TR20 and Tn90p measure night high temperature. The inter-decadal variation of TR20 is obvious in the southwest of MP, and there is no obvious inter-decadal change in other regions. The regions with obvious Tn90p changes are mainly concentrated in the southwest (period 1 to 2) and southeast (period 2 to 3) of MP, mainly within the scope of Inner Mongolia Autonomous Region. Based on the above analysis, it can be concluded that 1) The rise of both hot day and hot night indices is mainly concentrated in the south of MP. 2) the inter-decadal variation of the hot day indices in the northern part of the MP is greater, while the inter-decadal variation of the hot night indices in the southern part is greater at the stage when the extreme heat index changes

most violently, that is, from period 2 to period 3. 3) In the past two decades, the increase in extreme hot indices has been very small, and there has even been a slight decrease.

3.2.2 Extreme cold indices

Duzd in Mongolian means a cold winter, accompanied by strong winds and heavy snow. Studying the changes in the extreme cold indices can help us better understand the changes in the risk of Duzd on the MP. Indices exhibited in Fig. 7 are extreme cold indices and trends of these indices are shown in Table 4. The definition of Frost days (FD) and Icing days (ID0) are like that of SU and TR, and the definition of cold days (Tx10p) and cold nights (Tn10p) are like that of Tx90p and Tn90p. FD and ID0 showed downward trends of -2.94 days/decade and − 3.25 days/decade respectively, and Tx10p and Tn10p showed downward trends of -0.63%/decade and − 0.86%/decade, respectively. Cold spell duration index (CSDI) measure the number of days of abnormal cold, decreasing with a trend of -0.19 days/decade from 1981 to 2020. All the five indices showed significant descending trends during 1981–2020, suggesting that the frequency of extreme cold events on the MP has been decreasing both in frequency and duration since 1981.

Table 4
Trends and inter-decadal variation of extreme cold indices

	period 1	period 2	period 3	period 4	Slope
FD(day)	202.43	202.20	197.09	195.20	-2.94**
ID0(day)	123.84	117.98	117.60	115.53	-3.25**
TX10p(%)	10.38	8.58	8.73	8.21	-0.63**
TN10p(%)	10.86	8.51	8.19	7.61	-0.86**
CSDI(day)	4.10	1.63	2.99	2.68	-0.19**

Figure 8 shows the spatial pattern of trends of extreme cold indices (FD, ID, Tn10p, and Tx10p). FD decreased significantly on almost the entire MP and the decline of FD in the southern part of the MP is faster than in the northern part. ID0 decreased. Compared with FD, the change trend of ID0 in the southwest and east of the MP is not significant, mainly showing a significant downward trend in the middle of the MP. The spatial pattern of the change trend of Tx10p and Tn10p is similar, both decreasing significantly mainly in eastern MP, and increasing insignificantly in western MP.

Results in Table 4 also exhibit the decadal variation of extreme cold indices. These indices decreased the fastest from period 1 to period 2 except FD. ID0 decreased by 8.61 days from period 1 to period 2. Tn10p and Tx10p decreased intensely from period 1 to 2 with − 4.48% and − 3.3%, and changed little between the other three decades. From period 1 to period 2, the decrease in CSDI was also the largest, at 2.47 days. Different from other extreme cold indices, FD decreased fastest from period 2 to period 3, with an

average decrease of 5.10 days. We also calculated the difference of 4 extreme cold indices between adjacent periods and results is Shown in Fig. 9. The spatial pattern of inter-decadal changes in FD is significantly different from the other three indices. From period 1 to period 2, FD rose in the west of MP while the other three indices decreased in most parts of MP. From period 2 to period 3, the inter-decadal changes of Tx10p and Tn10p presented a similar spatial pattern, rising in the north and northeast of MP. The inter-decadal changes of all four indices are less significant from period 3 to period 4 compared with other two adjacent periods.

These findings suggest that changes in extreme cold indices can be used to better understand the risk of Duzd on the MP. Moreover, these results can be useful for policymakers and stakeholders in developing effective strategies to mitigate the impacts of extreme cold events and climate change on the MP. It is important to note that this study only focused on extreme cold indices and further research is needed to understand the changes in other climate variables that may also impact the risk of Duzd on the MP.

3.2.3 Extreme precipitation events

Figure 10 shows the changes of extreme precipitation indices and trends are shown in Table 5. Simple precipitation intensity index (SDII) and annual total precipitation in wet days (PRCPTOT) calculate wet season precipitation intensity and total wet season precipitation respectively. Consecutive dry days (CDD) and Consecutive wet days (CWD) calculated the longest consecutive dry and wet days in a year. heavy precipitation days (R10mm) and heavy precipitation (R95p) describe extreme precipitation intensity based on percentage and a fixed value respectively. All the indices decreased except CDD during 1981–2020, which means extreme precipitation on the MP decreased both in duration and intensity. All the results are shown in Table 1. It's worth noting extreme precipitation indices underwent significant decline around 2000 except CDD. The inter-annual changes of these indices returned to stability after 2000.

Table 5
Trends and inter-decadal variation of extreme precipitation indices

	period 1	period 2	period 3	period 4	Slope
SDII(mm/day)	62.09	59.87	53.39	53.00	-3.30**
R10mm(days)	7.38	7.43	5.68	6.40	-0.44**
CDD(days)	52.69	57.04	54.98	59.28	2.12**
CWD(days)	5.91	5.98	5.08	5.29	-0.24**
R95p(mm)	51.81	50.61	40.32	42.27	-3.57**

The decadal variation of different extreme precipitation indices is explicit and approximately consistent. Based on the analysis of the results in Table 4, almost all the indices increased slightly in the period 2 compared with the period 1 and decreased intensely in the period 3 compared with period 2. Compared

with the period 3, most indices showed slight decreases in period 4. CDD seemed to be different, keeping increasing from period 1 to period 3. The results indicate that the extreme precipitation in MP has been decreasing since the first period and the magnitude of decline between the second and third periods is the largest.

Figure 11 shows the spatial pattern of trends of extreme precipitation indices from 1981 to 2020. SDII and PRCPTOT had similar spatial distribution, emerging significant descending trends in northern and northeastern MP. The places with drastic changes are mainly concentrated in the north and northeast of the MP. Compared with other indices, CWD and CDD are less spatial coherent. CWD mainly presents a downward trend in the northwest mountainous areas, while CDD mainly presents an upward trend on the central MP. R10mm and R95p mainly decreased in the northern and eastern MP and showed no obvious change trend in the southwest of the MP. In general, the changes in all extreme wet indices are not significant in the southwest of the MP, as it is a desert region with little annual precipitation.

Due to the similarity in the spatial pattern of inter-decadal variability of extreme precipitation indices, two indices, SDII and R10mm, were selected for analysis. Figure 12 shows the inter-decadal variation of SDII and R10mm. SDII increased in northeastern MP from period 1 to 2, in south western MP from period 2 to 3, and in central MP from period 3 to 4. R10mm also exhibits significant inter-decadal fluctuations in the eastern MP, decreasing from period 2 to period 3 and increasing from period 3 to period 4. Overall, the inter-decadal fluctuations of extreme precipitation indices are greater in areas with high precipitation levels.

3.3 Relationship between extreme indices and circulation indices

In order to attribute the change of extreme indices, we conducted stepwise regression between ocean–atmosphere oscillations indices and extreme indices. All the indices had been standardized to compare the impact of different circulation indices. At first, 15 circulation indices were selected and after stepwise regression was carried out, we picked 4 most significant indices and excluded the rest indices. The coefficients of stepwise regression are shown in Table 6. Backslash indicate that the index is removed in stepwise regression. All the coefficients are significant at 0.05 confidence level. Atlantic Meridional Mode (AMM) mainly showed negative correlation with extreme precipitation indices and was excluded in the stepwise regression with temperature indices. AMM may have an impact on precipitation by affecting the East Asian jet stream. Arctic Oscillation (AO) only showed negative correlation with extreme cold indices It has been proved that AO is closely related to Eurasian winter temperatures (Thompson and Wallace 2000). Oppositely, Pacific Decadal Oscillation (PDO) only showed negative correlation with extreme hot indices and FD. It has been found that there is a good correlation between PDO and the extreme high temperature in North China (Zhang et al. 2020). WHWP was selected as an independent variable in every stepwise regression with extreme temperature indices, while didn't show significant relevance with extreme precipitation indices. The coefficient of Western Hemisphere Warm Pool (WHWP) is positive when the dependent variable of the equation is extreme hot indices and negative when extreme cold

indices. It has been found that due to the westward propagation of Rossby waves related to WHWP-SST, WHWP contributed to the climate variability in the Western North Pacific (Park et al. 2019). The results suggest that the changes of temperature indices and precipitation indices are affected by different ocean–atmosphere oscillation patterns. Adjust R^2 represents the degree to which the independent variable explains the dependent variable in stepwise regression. In general, the adjust R^2 is higher when the independent variable is a temperature index than when the independent variable is a precipitation index. However, all the adjust R^2 aren't greater than 0.51, indicating that the change of extreme indices is only partially attributable to large-scale circulation.

Table 6
Results of stepwise regression between extreme climate indices and circulation indices

	AMM	AO	PDO	WHWP	Adjust R^2
SU25(days)	\	\	-0.51	0.48	0.36
TR20(days)	\	\	-0.49	0.45	0.32
TX90p(%)	\	\	-0.31	0.68	0.44
TN90p(%)	\	\	-0.34	0.73	0.52
WSDI(days)	\	\	\	0.44	0.17
FD(days)	0.32	\	0.47	-0.76	0.41
ID0(days)	\	-0.47	\	-0.53	0.41
TN10p(%)	\	-0.63	\	-0.44	0.51
TX10p(%)	\	-0.62	\	-0.26	0.39
CSDI(days)	\	\	\	-0.4	0.14
SDII(mm/day)	-0.41	\	\	\	0.14
PRCPTOT(mm)	-0.4	\	\	\	0.14
CWD(days)	-0.38	\	\	\	0.12
R10mm(days)	-0.38	\	\	\	0.12
R95p(mm)	-0.37	\	\	\	0.11

4 Conclusion

The extreme climate of MP has changed significantly in 1981–2020. Based on the ERA5 reanalysis dataset to calculate the extreme climate indices, this study mainly draws the following conclusions:

1) Changes of temperature and precipitation on the MP.

Average, maximum and minimum temperature showed increasing trends during 1981–2020, with rates of 0.40 ℃/decade, 0.37 ℃/decade, and 0.38 ℃/decade, respectively. From the perspective of spatial pattern, average temperature significantly increased during 1981–2020 on the almost entire MP at 0.05 confidence level and insignificantly decreased on small part of the southwestern MP. The rising trend of temperature on the central MP, where the Khangai Mountains are located, is higher than that in other regions. The lower the temperature, the faster and more significant the increase. Total precipitation ranged from 240 mm to 400 mm on the MP during 1981–2020 and presented a changing pattern of inter-decadal fluctuations. Precipitation significantly decreased at 0.05 confidence level on the northern, northwestern and eastern MP and increased insignificantly on the southwestern MP. Northern and northeastern parts of the MP are facing more severe threat of water shortage.

2) Changes of extreme hot indices on the MP

This study has studied the inter-annual and inter-decadal changes of extreme hot indices, extreme cold indices and extreme precipitation indices on the MP in the past 40 years. The degree of extreme heat events facing the MP has gradually increased over the past 40 years. The five indices used to characterize extreme hot events, including Summer days, Tropical nights, Warm days, Warm nights, and Warm spell duration index, have all increased significantly during 1981–2020. The spatial pattern of the inter-annual variation trends of Summer days, Warm days, and Warm nights is similar, increasing significantly on almost the entire MP. The magnitude of upward trends of these three indices in the central part of the MP is higher than those around the MP. Therefore, the probability of the central MP facing extreme hot events in the future is higher than that of other regions. Unlike the other three indices, Tropical nights only increased significantly on the southwestern MP, where deserts are located, and showed no obvious trend in other parts of the MP.

As for inter-decadal variation, nearly all the extreme hot indices rose the fastest from period 2 to period 3. The inter-decadal variation of the hot day indices in the northern part of the MP is greater, while the inter-decadal variation of the hot night indices in the southern part is greater at the stage when the extreme heat index changes most violently, that is, from period 2 to period 3. In the past two decades, the increase in extreme hot indices has been very small, and there has even been a slight decrease.

3) Changes of extreme cold indices on the MP

The frequency and duration of extreme cold events have been decreasing since 1981. This is supported by the significant downward trends exhibited by all five extreme cold indices (Frost days, Icing days, cold days, cold nights, and cold spell duration index) over the period of 1981–2020. The fastest decrease in extreme cold indices occurred from period 1 to period 2, except for FD which decreased the fastest from period 2 to period 3.

Spatial patterns of the trends in extreme cold indices indicate that the decline in Frost days was significant on almost the entire Mongolian Plateau (MP), with the decline in the southern part being faster than in the northern part. Icing days showed a significant downward trend mainly in the middle of the MP.

Cold days and cold nights decreased significantly in the eastern MP, and increased insignificantly in the western MP. The inter-decadal changes in FD differed significantly from the other three indices, as they rose in the west of MP from period 1 to period 2.

4) Changes of extreme precipitation indices on the MP

The results showed that all the extreme precipitation indices decreased except CDD during the period of 1981–2020, indicating that extreme precipitation on the MP decreased both in duration and intensity. The spatial pattern of trends of extreme precipitation indices from 1981 to 2020 was also examined. SDII and PRCPTOT had similar spatial distribution, with significant descending trends in northern and northeastern MP. CWD mainly presented a downward trend in the northwest mountainous areas, while CDD mainly presented an upward trend on the central MP. R10mm and R95p mainly decreased in the northern and eastern MP and showed no obvious change trend in the southwest of the MP. The changes in all extreme wet indices were not significant in the southwest of the MP due to its desert region with little annual precipitation.

In terms of decadal variation of different extreme precipitation indices, almost all the indices increased slightly in period 2 compared with period 1 and decreased intensely in period 3 compared with period 2. Compared with period 3, most indices showed slight decreases in period 4. CDD kept increasing from period 1 to period 3, indicating that extreme precipitation in MP has been decreasing since the first period, and the magnitude of decline between the second and third periods is the largest. The inter-decadal fluctuations of extreme precipitation indices were greater in areas with high precipitation levels. Based on the analysis, it can be concluded that extreme precipitation in the MP has been decreasing, and the magnitude of decline between the second and third periods is the largest.

5) Relationships between extreme climate indices and atmospheric circulation indices.

We conducted stepwise regression between extreme climate indices and atmospheric circulation indices. The results revealed that extreme precipitation indices were negatively correlated with Atlantic Meridional Mode (AMM) and positively correlated with Western Hemisphere Warm Pool (WHWP). However, WHWP did not show significant relevance with extreme precipitation indices. On the other hand, Arctic Oscillation (AO) only showed negative correlation with extreme cold indices, while Pacific Decadal Oscillation (PDO) only showed negative correlation with extreme hot indices and FD. The results suggest that changes in temperature and precipitation indices are influenced by different ocean-atmosphere oscillation patterns. The adjust R^2 values indicate that the independent variables explain the dependent variables to a certain extent. Nevertheless, the adjust R^2 values were relatively low, suggesting that the changes in extreme indices are only partially attributable to large-scale circulation. Overall, the results of this study enhance our understanding of the complex relationships between extreme precipitation indices and ocean-atmosphere oscillations.

Declarations

Acknowledgments This study was supported by the National Natural Science Foundation of China (Grant No. 42230506).

Funding The authors declare that no funds were received during the preparation of this manuscript.

Competing Interests The authors have no relevant financial or non-financial interests to disclose.

Author Contributions Guoying Zhu conducted the analysis and wrote the main manuscript text. Xinyi Zhao conceptualized and revised the paper.

Data Availability Data used in this study including station data in Inner Mongolia, China and Mongolia, and ERA5 reanalysis dataset. Station data in Inner Mongolia is available from National Meteorological Science Data Center (http://data.cma.cn/). Station data in Mongolia is available from Global Historical Climatology Network (https://www.ncei.noaa.gov/access/metadata/landing-page/bin/iso?id=gov.noaa.ncdc%3AC00861). ERA reanalysis data is available from European Centre for Medium-Range Weather Forecasts (https://www.ecmwf.int/en/forecasts/dataset/ecmwf-reanalysis-v5).

References

1. Alexander, L. V., X. Zhang, T. C. Peterson, J. Caesar, B. Gleason, A. M. G. Klein Tank, M. Haylock, D. Collins, B. Trewin, F. Rahimzadeh, A. Tagipour, K. Rupa Kumar, J. Revadekar, G. Griffiths, L. Vincent, D. B. Stephenson, J. Burn, E. Aguilar, M. Brunet, M. Taylor, M. New, P. Zhai, M. Rusticucci and J. L. Vazquez-Aguirre (2006). Global observed changes in daily climate extremes of temperature and precipitation. J Geophys Res 111(D5).https://doi.org/10.1029/2005jd006290
2. Bayasgalan, B., R. Mijiddorj, P. Gomboluudev, D. Oyunbaatar and L. Molomjamts (2009). Climate change and sustainable livelihood of rural people in Mongolia.
3. Bell, J. E., C. L. Brown, K. Conlon, S. Herring, K. E. Kunkel, J. Lawrimore, G. Luber, C. Schreck, A. Smith and C. Uejio (2018). Changes in extreme events and the potential impacts on human health. J Air Waste Manage Assoc 68(4): 265-287.https://doi.org/10.1080/10962247.2017.1401017
4. Beniston, M., D. B. Stephenson, O. B. Christensen, C. A. T. Ferro, C. Frei, S. Goyette, K. Halsnaes, T. Holt, K. Jylhä, B. Koffi, J. Palutikof, R. Schöll, T. Semmler and K. Woth (2007). Future extreme events in European climate: an exploration of regional climate model projections. Clim Change 81(S1): 71-95.https://doi.org/10.1007/s10584-006-9226-z
5. Chen, J. and J. Zhao (2017). Trends of Extreme Weather Events in Inner Mongolia during the Period of 1960 -2014. Arid Zone Res 34(5): 997-1009
6. Chun, L., F. Qin, L. Bao, Y. Na, Y. Bao and S. Bao (2019). Spatiotemporal Variation of Extreme Precipitation Indices in Inner Mongolia in Recent 55 Years. Arid Zone Res 36(4): 963-972
7. Cui, D., C. Wang and J. Santisirisomboon (2019). Characteristics of extreme precipitation over eastern Asia and its possible connections with Asian summer monsoon activity. Int J Climatol 39(2): 711-723.https://doi.org/10.1002/joc.5837

8. Dashkhuu, D., J. P. Kim, J. A. Chun and W.-S. Lee (2015). Long-term trends in daily temperature extremes over Mongolia. Weather Clim Extremes 8: 26-33.https://doi.org/10.1016/j.wace.2014.11.003
9. Du, J., H. Lu and J. Jian (2013). Variations of extreme air temperature events over Tibet from 1961 to 2010. Acta Geogr Sin 68(9): 1269-1280
10. Easterling, D. R., G. A. Meehl, C. Parmesan, S. A. Changnon, T. R. Karl and L. O. Mearns (2000). Climate Extremes: Observations, Modeling, and Impacts. Science 289(5487): 2068-2074.https://doi.org/doi:10.1126/science.289.5487.2068
11. Fernández-Giménez, M. E., B. Batkhishig and B. Batbuyan (2012). Cross-boundary and cross-level dynamics increase vulnerability to severe winter disasters (dzud) in Mongolia. Glob Environ Change 22(4): 836-851.https://doi.org/10.1016/j.gloenvcha.2012.07.001
12. Fischer, E. M., S. Sippel and R. Knutti (2021). Increasing probability of record-shattering climate extremes. Nat Clim Change 11(8): 689-695.https://doi.org/10.1038/s41558-021-01092-9
13. Fu, G., N. R. Viney, S. P. Charles and J. Liu (2010). Long-Term Temporal Variation of Extreme Rainfall Events in Australia: 1910–2006. J Hydrometeorol 11(4): 950-965.https://doi.org/10.1175/2010jhm1204.1
14. Fu, G., J. Yu, X. Yu, R. Ouyang, Y. Zhang, P. Wang, W. Liu and L. Min (2013). Temporal variation of extreme rainfall events in China, 1961–2009. J Hydrol 487: 48-59.https://doi.org/10.1016/j.jhydrol.2013.02.021
15. Hajat, S., B. Armstrong, M. Baccini, A. Biggeri, L. Bisanti, A. Russo, A. Paldy, B. Menne and T. Kosatsky (2006). Impact of High Temperatures on Mortality. Epidemiology 17(6): 632-638.https://doi.org/10.1097/01.ede.0000239688.70829.63
16. He, L., B. Xue, B. Wang, C. Liu, D. Gimeno Ruiz de Porras, G. L. Delclos, M. Hu, B. Luo and K. Zhang (2022). Impact of high, low, and non-optimum temperatures on chronic kidney disease in a changing climate, 1990–2019: A global analysis. Environ Res 212.https://doi.org/10.1016/j.envres.2022.113172
17. Iijima, Y. and M. E. Hori (2016). Cold air formation and advection over Eurasia during “dzud” cold disaster winters in Mongolia. Nat Hazards 92(S1): 45-56.https://doi.org/10.1007/s11069-016-2683-4
18. Kemp, L., C. Xu, J. Depledge, K. L. Ebi, G. Gibbins, T. A. Kohler, J. Rockstrom, M. Scheffer, H. J. Schellnhuber, W. Steffen and T. M. Lenton (2022). Climate Endgame: Exploring catastrophic climate change scenarios. Proceedings of the National Academy of Sciences of the United States of America 119(34): e2108146119.https://doi.org/10.1073/pnas.2108146119
19. Kruger, A. C. and S. S. Sekele (2013). Trends in extreme temperature indices in South Africa: 1962-2009. Int J Climatol 33(3): 661-676.https://doi.org/10.1002/joc.3455
20. Li, C., W. Leal Filho, J. Wang, H. Fudjumdjum, M. Fedoruk, R. Hu, S. Yin, Y. Bao, S. Yu and J. Hunt (2018). An Analysis of Precipitation Extremes in the Inner Mongolian Plateau: Spatial-Temporal Patterns, Causes, and Implications. Atmosphere 9(8).https://doi.org/10.3390/atmos9080322

21. Li, W., L. Duan, T. Liu, Geriletu, R. Gao, S. Buren and C. Yu (2017). Spatio-temporal variations of extreme precipitation from 1961 to 2015 in the eastern inland river basin of Inner Mongolian Plateau. Resources Science 39(11): 2153-2165
22. Li, Y., S. Tong, Y. Bao, E. Guo and Y. Bao (2020). Prediction of Droughts in the Mongolian Plateau Based on the CMIP5 Model. Water 12(10).https://doi.org/10.3390/w12102774
23. Liu, Z., Z. Yao, H. Huang, B. Batjav and R. Wang (2019). Evaluation of Extreme Cold and Drought over the Mongolian Plateau. Water 11(1).https://doi.org/10.3390/w11010074
24. Lorenz, R., Z. Stalhandske and E. M. Fischer (2019). Detection of a Climate Change Signal in Extreme Heat, Heat Stress, and Cold in Europe From Observations. Geophys Res Lett 46(14): 8363-8374.https://doi.org/10.1029/2019gl082062
25. Mann, R., A. Gupta, A. Dhorde and S. Sharma (2023). Observed trends and coherent changes in daily rainfall extremes over Greater Mumbai, 1985-2020. Theor Appl Climatol https://doi.org/10.1007/s00704-022-04354-4
26. Mason, S. J., P. R. Waylen, G. M. Mimmack, B. Rajaratnam and J. M. Harrison (1999). Changes in extreme rainfall events in South Africa. Clim Change 41(2): 249-257.https://doi.org/10.1023/a:1005450924499
27. Park, J. H., J. S. Kug, S. I. An and T. Li (2019). Role of the western hemisphere warm pool in climate variability over the western North Pacific. Clim Dyn 53(5-6): 2743-2755.https://doi.org/10.1007/s00382-019-04652-0
28. Roldán, E., M. Gómez, M. R. Pino and J. Díaz (2014). The impact of extremely high temperatures on mortality and mortality cost. Int J Environ Health Res 25(3): 277-287.https://doi.org/10.1080/09603123.2014.938028
29. Rusticucci, M. (2012). Observed and simulated variability of extreme temperature events over South America. Atmos Res 106: 1-17.https://doi.org/10.1016/j.atmosres.2011.11.001
30. Seneviratne, S. I., X. Zhang, M. Adnan, W. Badi, C. Dereczynski, A. Di Luca, S. Ghosh, I. Iskandar, J. Kossin, S. Lewis, F. Otto, I. Pinto, M. Satoh, S. M. Vicente-Serrano, M. Wehner and B. Zhou (2021). Weather and Climate Extreme Events in a Changing Climate. Climate Change 2021: The Physical Science Basis. Contribution of Working Group I to the Sixth Assessment Report of the Intergovernmental Panel on Climate Change. V. Masson-Delmotte, P. Zhai, A. Pirani et al. Cambridge, United Kingdom and New York, NY, USA, Cambridge University Press: 1513–1766.
31. Thompson D W J, Wallace J M, 2000. Annular modes in the extratropical circulation.Part : month-to-month variability[J]. J Climate, 13(5): 1000-1016. https://doi.org/10.1175/1520-0442(2000)013%3C1000:AMITEC%3E2.0.CO;2
32. Wang, L., Z.-J. Yao, L.-G. Jiang, R. Wang, S.-S. Wu and Z.-F. Liu (2016). Changes in Climate Extremes and Catastrophic Events in the Mongolian Plateau from 1951 to 2012. J Appl Meteorol Climatol 55(5): 1169-1182.https://doi.org/10.1175/jamc-d-14-0282.1
33. Xu, X., Y. Du, J. Tang and Y. Wang (2011). Variations of temperature and precipitation extremes in recent two decades over China. Atmos Res 101(1-2): 143-

154.https://doi.org/10.1016/j.atmosres.2011.02.003

34. Yan, G., F. Qi, L. Wei, L. Aigang, W. Yu, Y. Jing, C. Aifang, W. Yamin, S. Yubo, L. Li and M. Qianqian (2015). Changes of daily climate extremes in Loess Plateau during 1960–2013. Quat Int 371: 5-21.https://doi.org/10.1016/j.quaint.2014.08.052
35. Yan, H., W. Chen, F. Yang, J. Liu, Y. Hu and Y. Ji (2014). The spatial and temporal analysis of extreme climatic events in Inner Mongolia during the past 50 years. Geogr Res 33(1): 13-22
36. You, L., X. Dai and Y. Zhang (2010). Extreme Precipitation Events in Inner Mongolia in 1961-2008. Adv Clim Chang Res 6(6): 411-416
37. Zhang, A. and X. Zhao (2022). Changes of precipitation pattern in China: 1961–2010. Theor Appl Climatol 148(3-4): 1005-1019.https://doi.org/10.1007/s00704-022-03986-w
38. Zhang, G. W., G. Zeng, C. Li and X. Y. Yang (2020). Impact of PDO and AMO on interdecadal variability in extreme high temperatures in North China over the most recent 40-year period. Clim Dyn 54(5-6): 3003-3020.https://doi.org/10.1007/s00382-020-05155-z
39. Zhang, X., E. Aguilar, S. Sensoy, H. Melkonyan, U. Tagiyeva, N. Ahmed, N. Kutaladze, F. Rahimzadeh, A. Taghipour, T. H. Hantosh, P. Albert, M. Semawi, M. Karam Ali, M. H. Said Al-Shabibi, Z. Al-Oulan, T. Zatari, I. Al Dean Khelet, S. Hamoud, R. Sagir, M. Demircan, M. Eken, M. Adiguzel, L. Alexander, T. C. Peterson and T. Wallis (2005). Trends in Middle East climate extreme indices from 1950 to 2003. J Geophys Res 110(D22).https://doi.org/10.1029/2005jd006181

Figures

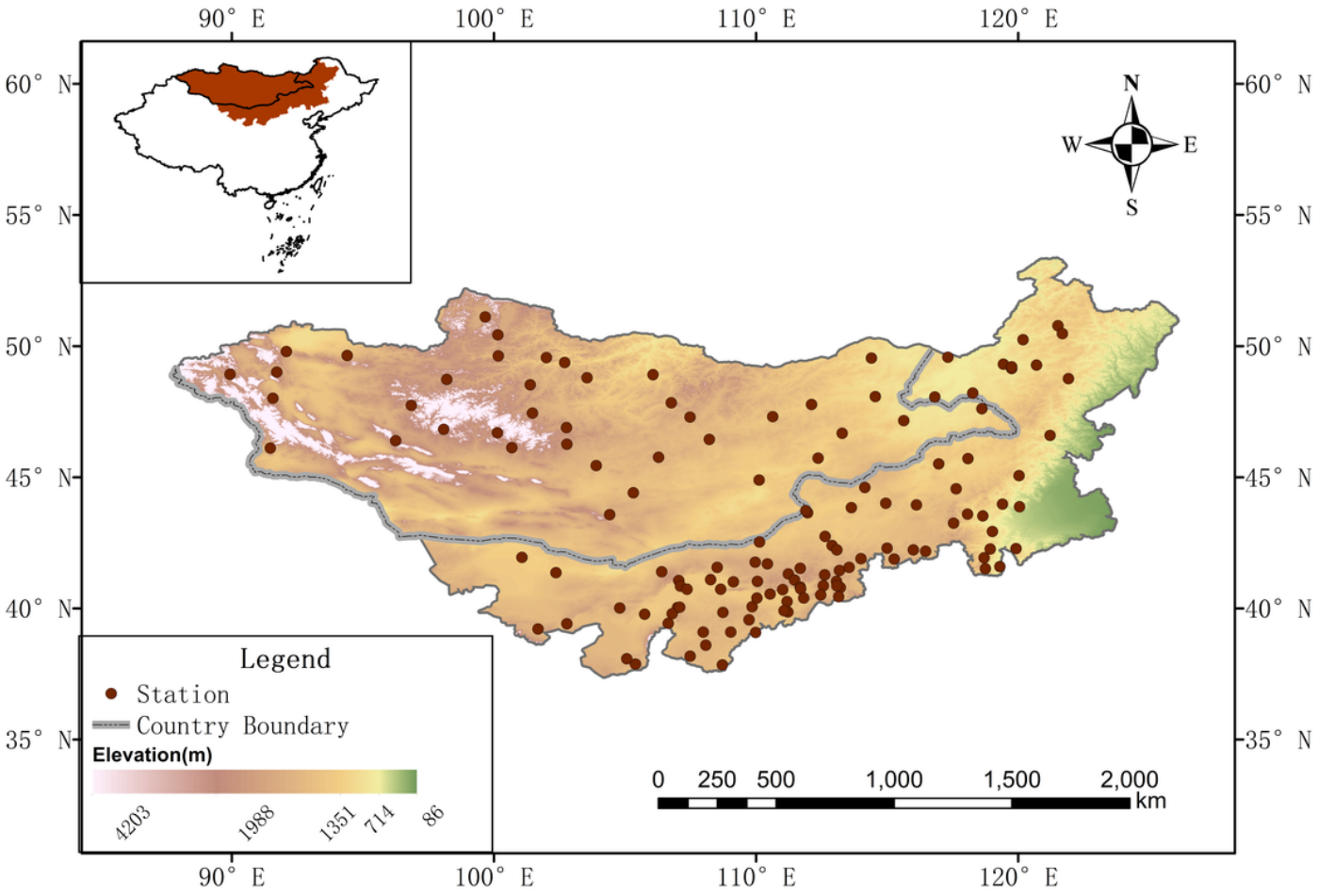

Figure 1

Elevation of Mongolia Plateau and spatial distribution of meteorological stations.

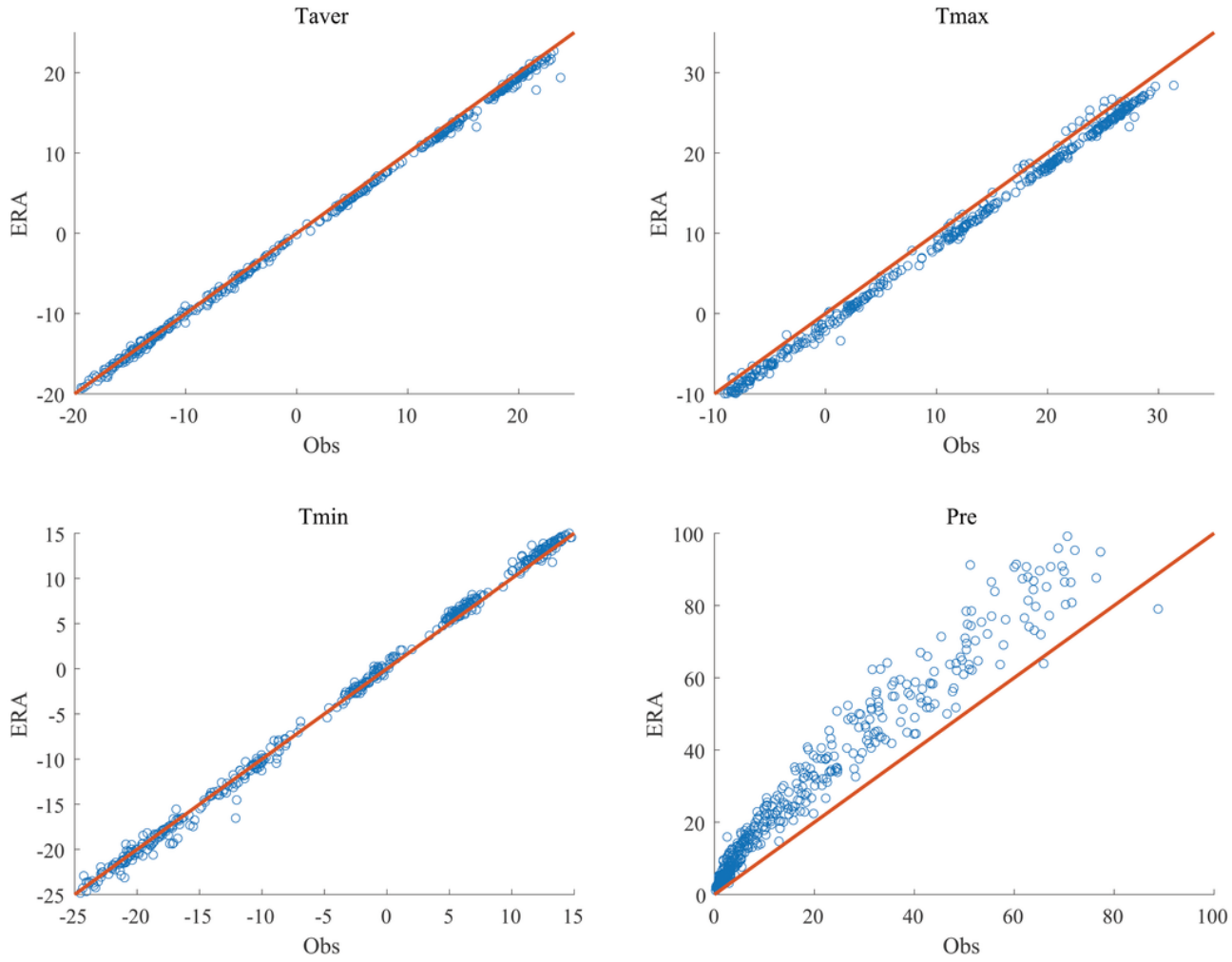

Figure 2

Scatter plots of observation data and ERA5 reanalysis dataset in average temperature, maximum temperature, minimum temperature and precipitation.

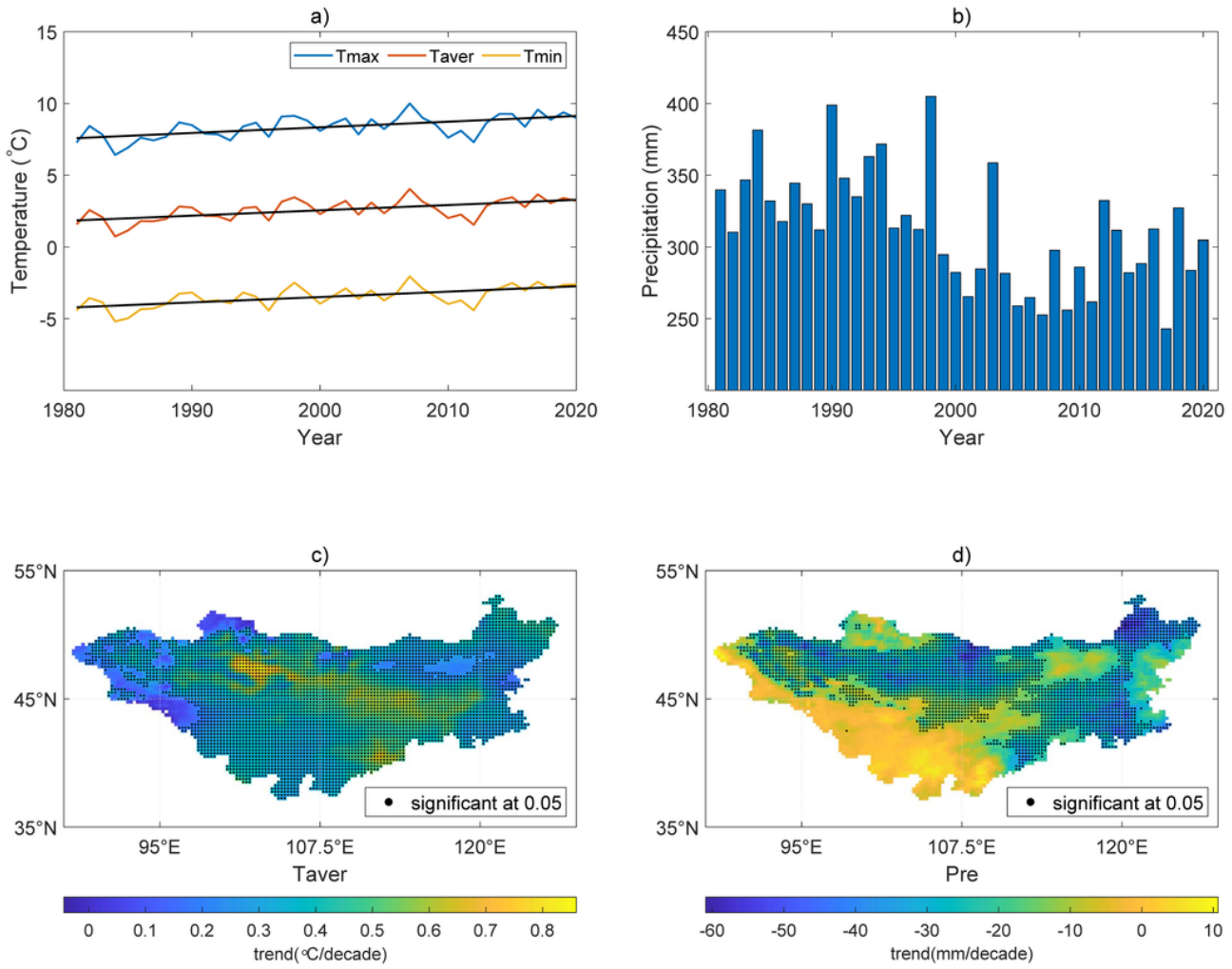

Figure 3

Temporal changes of average, maximum, and minimum temperature (a) and total precipitation (b) and spatial distribution of trends in average temperature (c) and total precipitation (d).

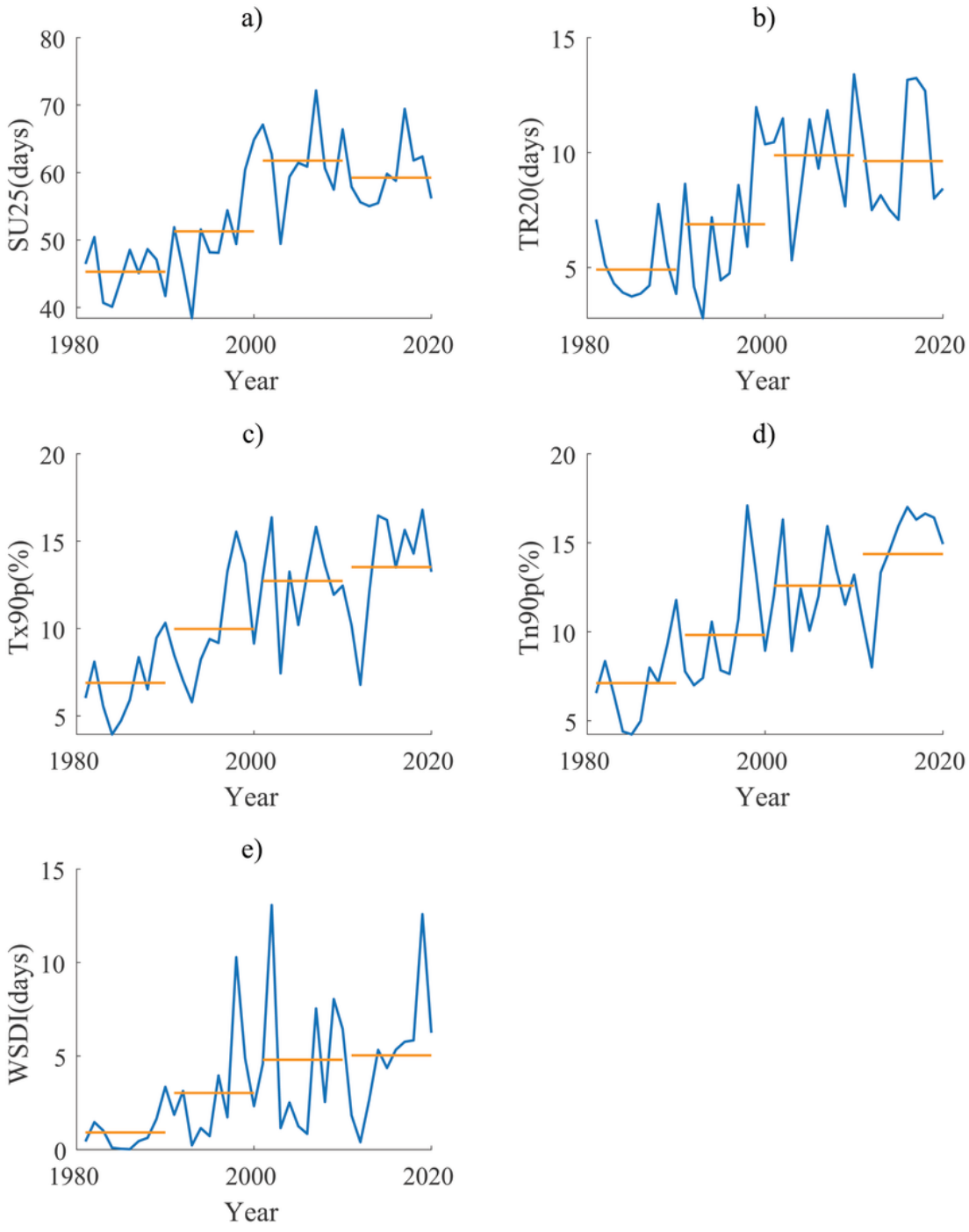

Figure 4

Temporal changes of extreme hot indices

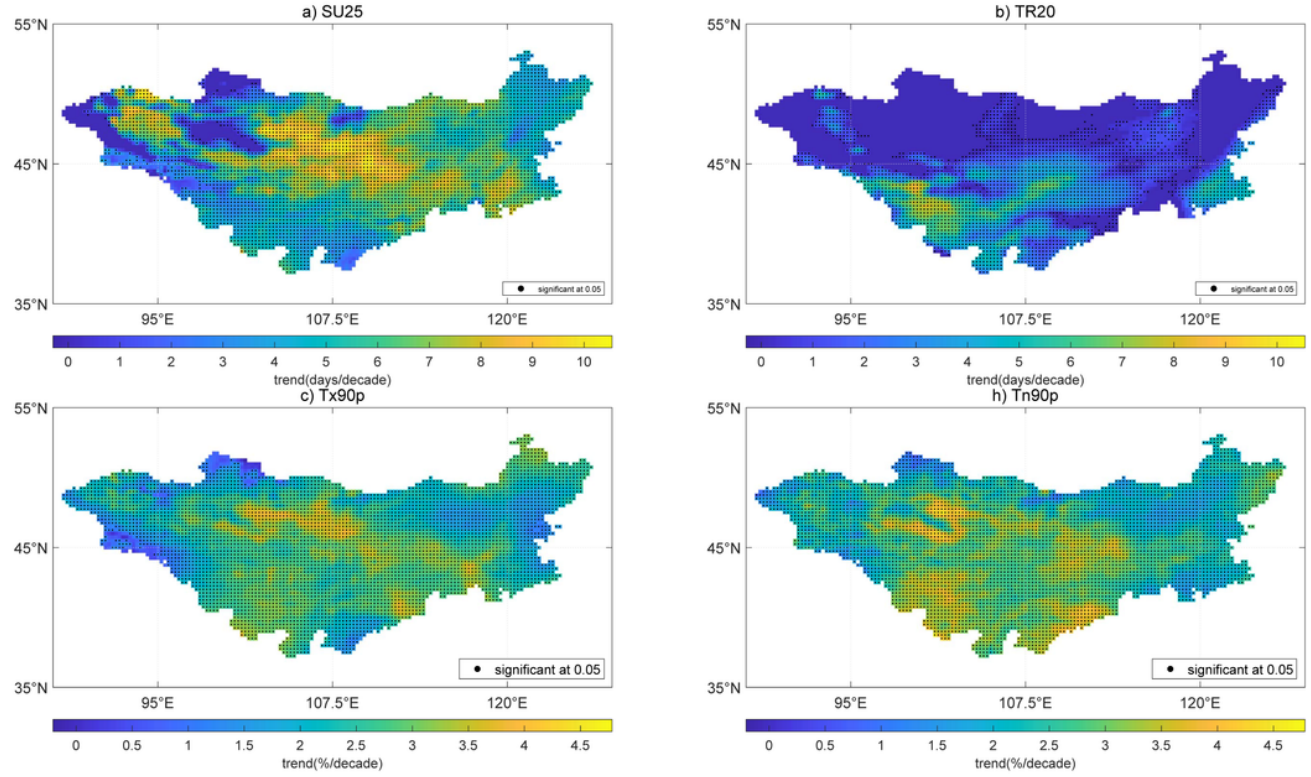

Figure 5

Spatial pattern of trends of extreme hot indices

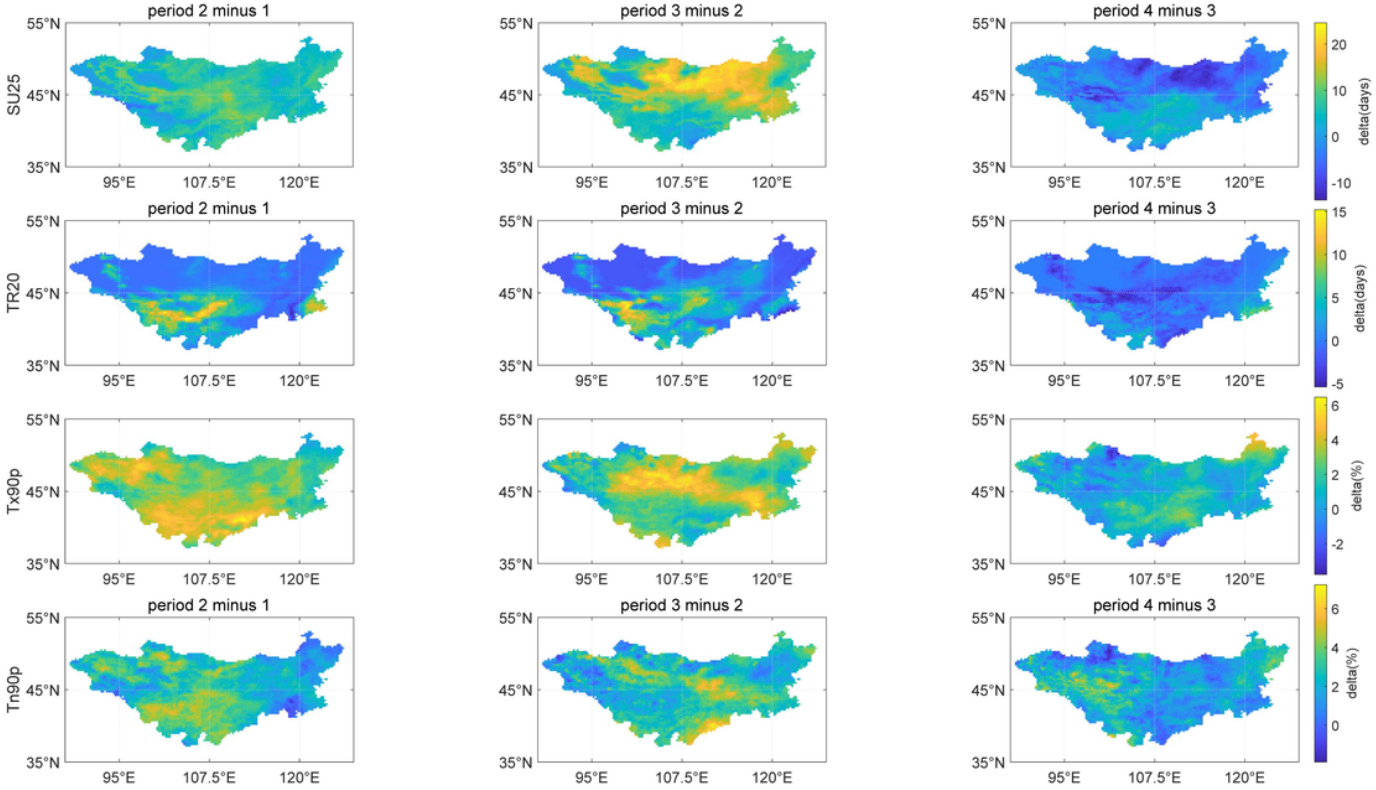

Figure 6

Spatial difference of extreme hot indices between two adjacent periods

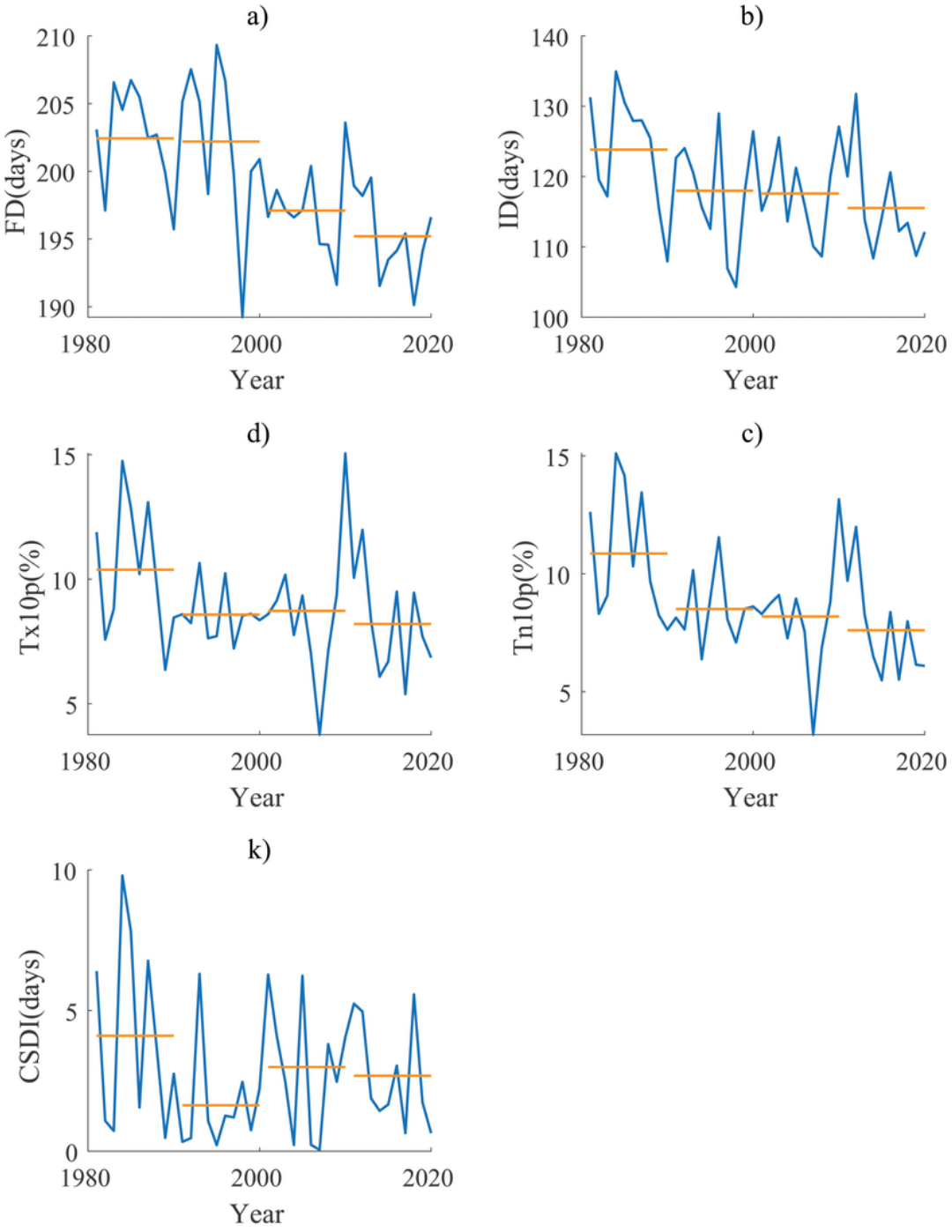

Figure 7

Temporal changes of extreme cold indices

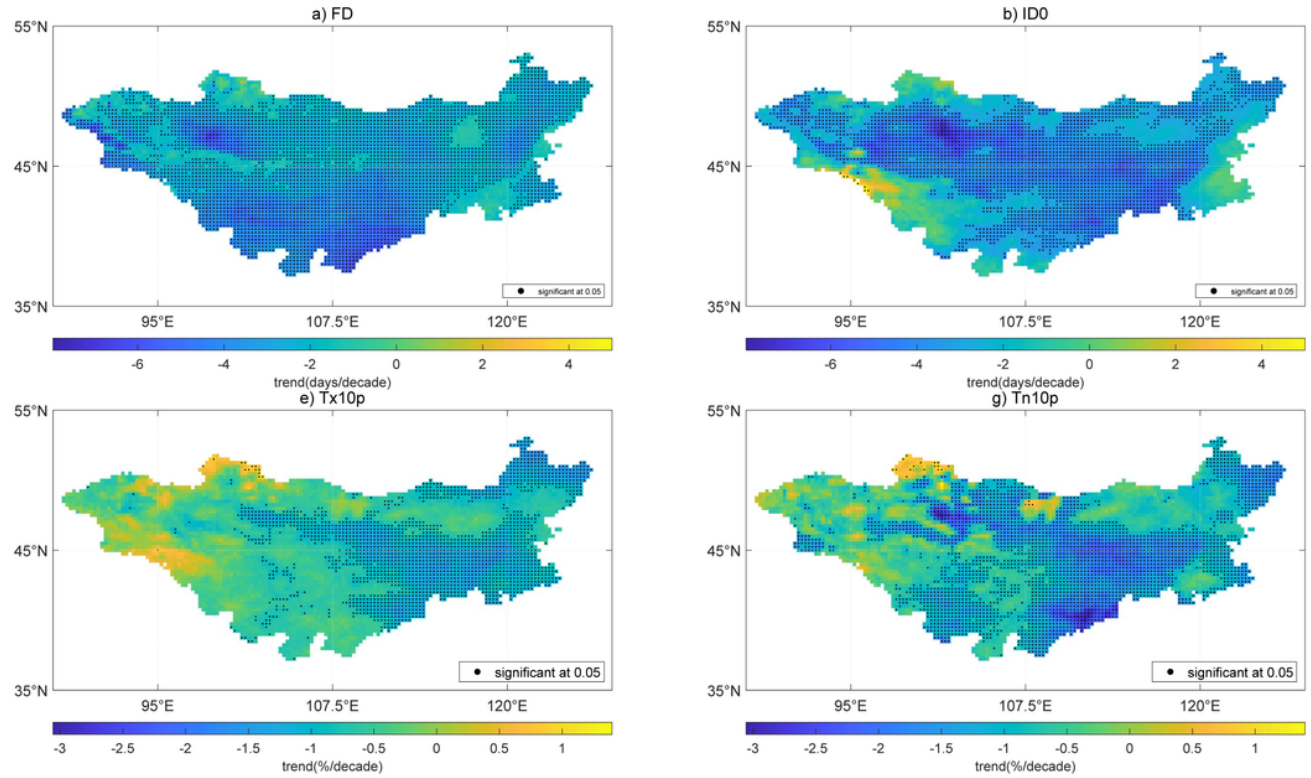

Figure 8

Spatial pattern of trends of extreme cold indices

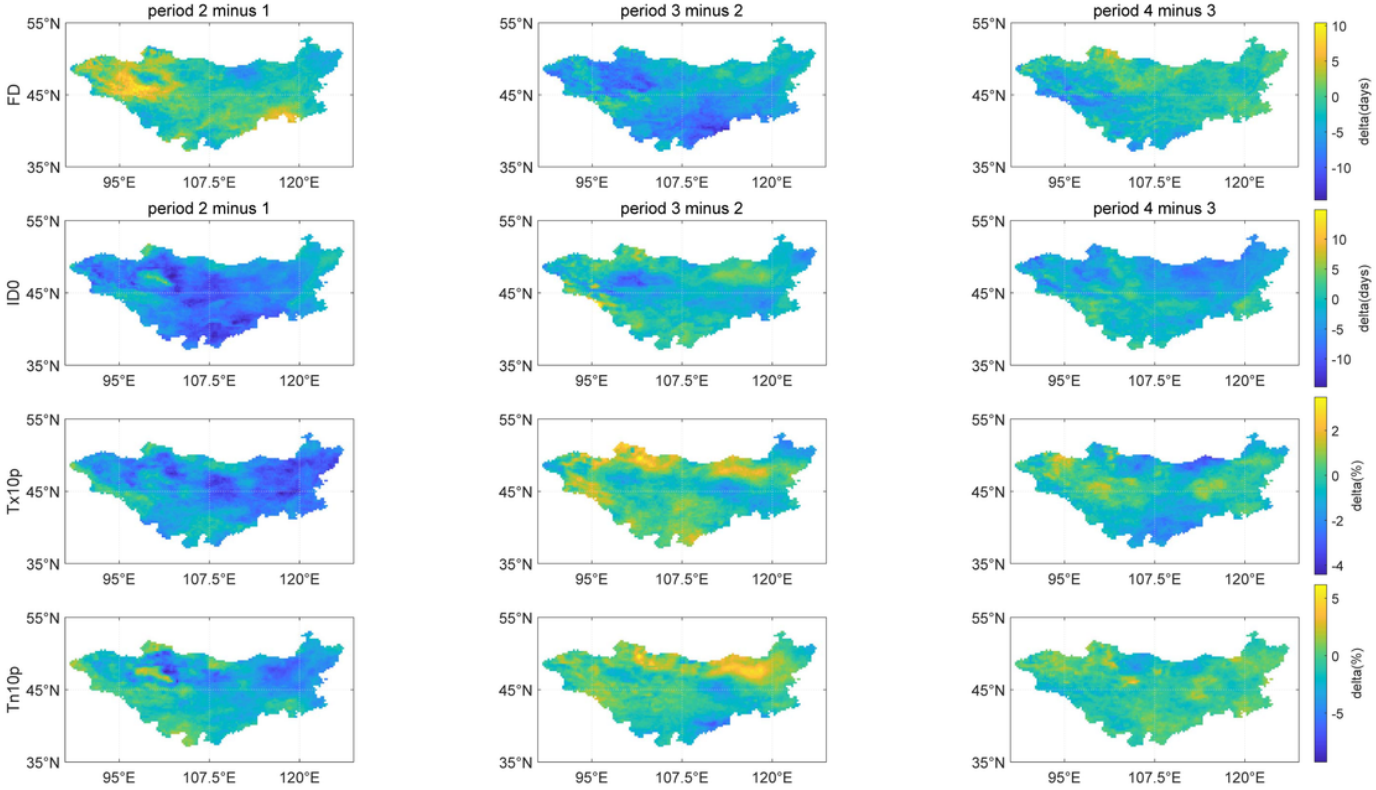

Figure 9

Spatial difference of extreme cold indices between two adjacent periods

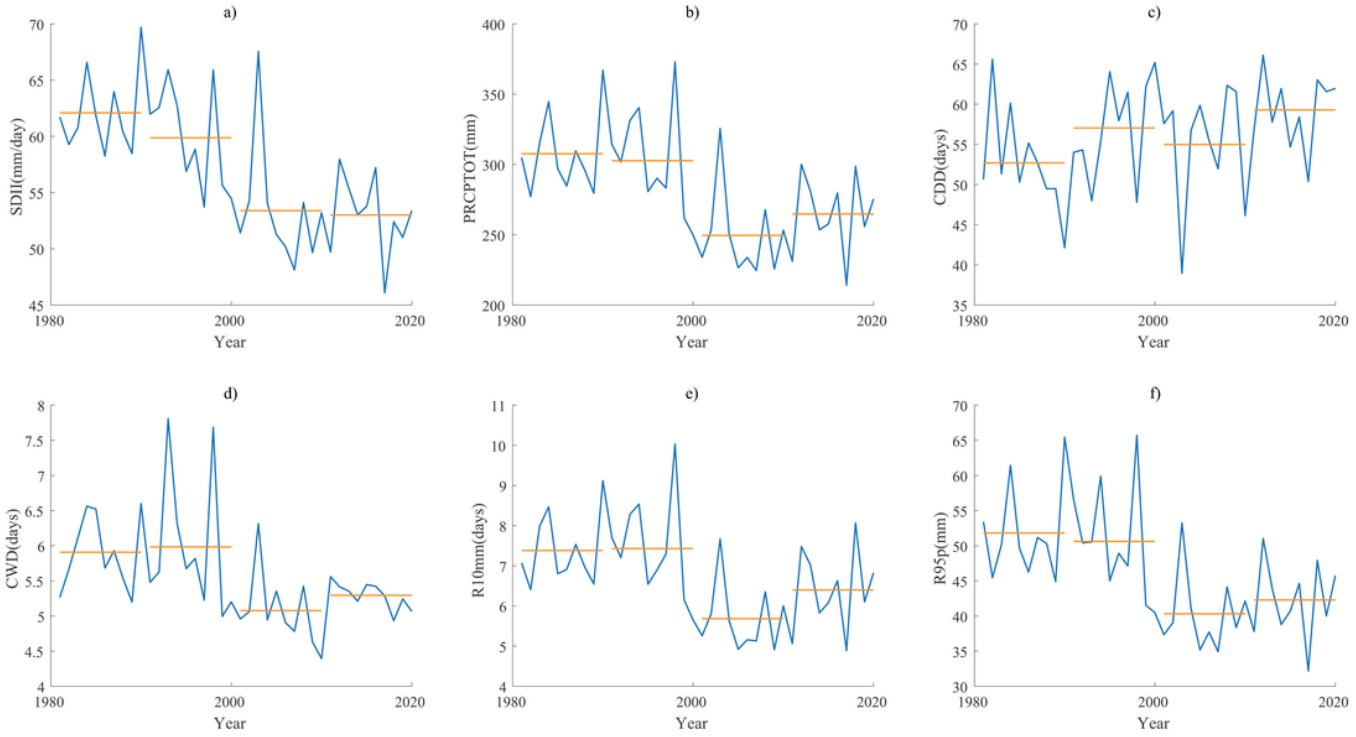

Figure 10

Temporal changes of extreme precipitation indices

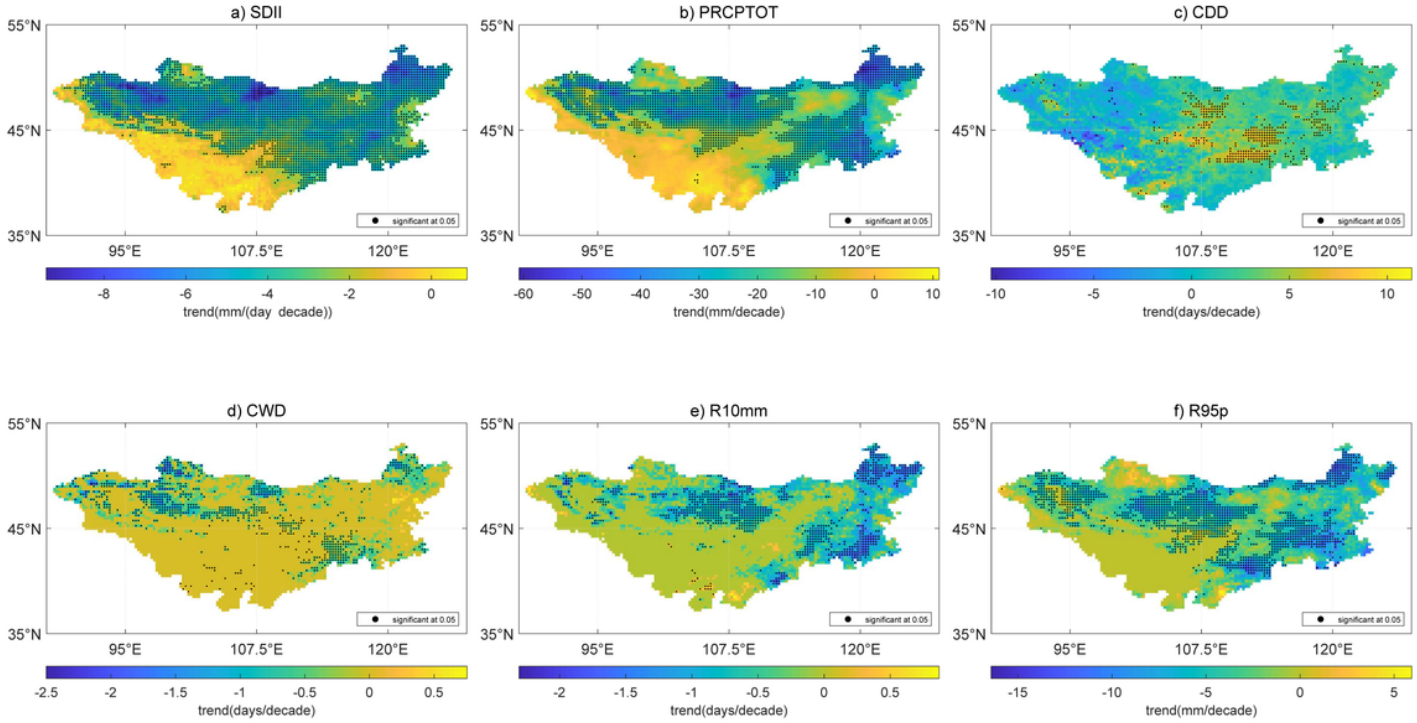

Figure 11

Spatial pattern of trends of extreme cold indices

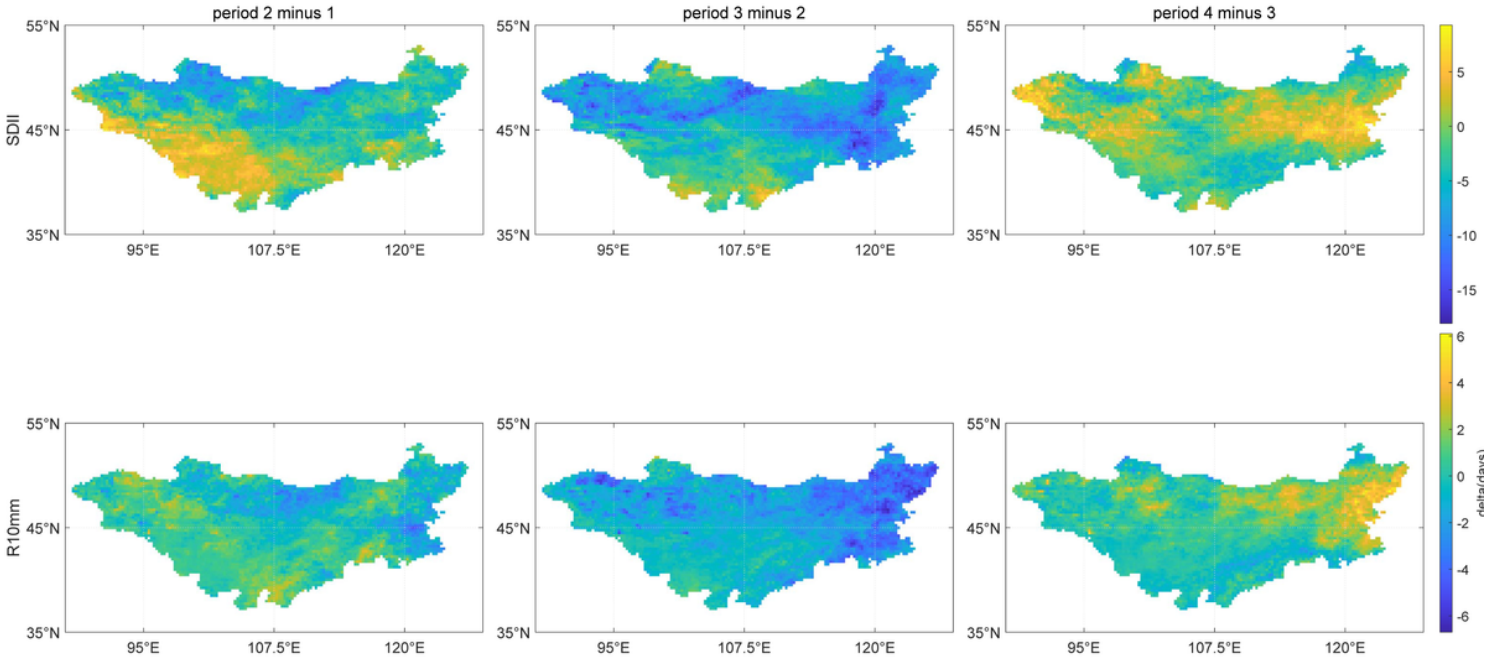

Figure 12

Spatial difference of extreme precipitation indices between two adjacent periods